

LABORATORY STUDY



# Nuclear paraspeckle assembly transcript 1 promotes the podocyte injury via targeting miR-23b-3p/B-cell lymphoma-2 interacting protein 3 like axis

Jing Wang<sup>a\*</sup>, Junpeng Luo<sup>b\*</sup>, Li Du<sup>c</sup>, Xin Shu<sup>d</sup>, Chengyu Guo<sup>a</sup> and Tanshi Li<sup>a</sup>

<sup>a</sup>Department of Emergency, The First Medical Center to Chinese People's Liberation Army General Hospital, Beijing, China;

<sup>b</sup>Department of Minimally Invasive Interventional Radiology, Sun Yat-sen University Cancer Center, State Key Laboratory of Oncology in South China, Collaborative Innovation Cancer for Cancer Medicine, Guangzhou, China; <sup>c</sup>The Institute of Radiation Medicine, The Academy of Military Medical Science, Beijing, China; <sup>d</sup>Department of Dermatology, Third Medical Center of Chinese, PLA General Hospital, Beijing, China

## ABSTRACT

**Background:** Given the reported effects of nuclear paraspeckle assembly transcript 1 (NEAT1) on kidney injury, a study is worth formulating to investigate whether and how NEAT1 impacts podocytes.

**Materials and methods:** A mouse podocyte injury model was established using the adriamycin (ADR)-induced mouse podocyte cell line (MPC5). The target relationships between NEAT1 and microRNA (miR)-23b-3p and between miR-23b-3p and Bcl-2 interacting protein 3 like (BNIP3L) were verified by dual-luciferase reporter assay and RNA immunoprecipitation assay. After ADR-induced MPC5 cells were transfected with NEAT1 overexpression plasmid (oe-NEAT1) or shNEAT1, the viability and apoptosis of MPC5 cells were evaluated by Cell Counting Kit-8 (CCK-8) assay and flow cytometry, respectively. The expressions of MPC5, miR-23b-3p, BNIP3L and the factors related to podocyte injury, apoptosis and epithelial-mesenchymal transition were determined using quantitative real-time polymerase chain reaction (qRT-PCR) and Western blot.

**Results:** NEAT1 was high-expressed in ADR-induced cell model. After transfection with oe-NEAT1, the expression of NEAT1, the levels of marker (Desmin) and apoptosis were promoted, while the viability and the levels of podocyte injury markers (WT1, Nephlin) were inhibited in ADR-induced cells. However, shNEAT1 generated the effects opposite to oe-NEAT1. Besides, miR-23b-3p competitively bound to NEAT1 and targeted BNIP3L. MiR-23b-3p inhibitor reversed the effect of shNEAT1, while its effect could be further offset by shBNIP3L. Furthermore, miR-23b-3p inhibitor affected mouse podocyte injury through downregulating Bcl-2 and E-cadherin levels and upregulating Cleaved-caspase-3, Bax, N-cadherin, Vimentin and Snail levels, but shBNIP3L did oppositely.

**Conclusion:** NEAT1 promotes the podocyte injury *via* targeting miR-23b-3p/BNIP3L axis.

## ARTICLE HISTORY

Received 27 August 2021

Revised 10 June 2022

Accepted 14 June 2022

## KEYWORDS



Podocyte injury; adriamycin (ADR); nuclear paraspeckle assembly transcript 1 (NEAT1); microRNA (miR)-23b-3p; B-cell lymphoma-2 (Bcl-2) interacting protein 3 like (BNIP3L)

## Introduction

Nephrotic syndrome (NS) is a pathological condition, with the manifestation of augmented protein content in the urine caused by increased permeability of the glomerular basement membrane [1]. Exposure to nephrotoxic drugs is one of the causes for NS development [2]. Podocyte is considered to be the key cell involved in the progress of NS [3]. As a kind of specialized epithelial cells in viscera, podocytes cover the basement membrane of glomerulus and form the filtration barrier [4], whose primary function is to maintain homeostasis when cells are subjected to stress [5].

Thus, the podocyte injury is a significant triggering factor of various glomerular diseases [6]. The mouse model of podocyte injury *in vitro* can be established by treating the mouse podocyte cell line MPC5 with adriamycin (ADR) with a reference to a relative recent research [7]. Notably, podocyte injury is also modulated by long non-coding RNAs (lncRNAs) and microRNAs (miRNAs, miRs) [8,9]. Despite improvement in our understanding of podocyte injury, the corresponding mechanism is still not fully explained.

lncRNAs refer to the molecules with over 200 nucleotides in length [10], serving principal roles in regulating human disease progression [11]. In the

**CONTACT** Tanshi Li  [litanshi\\_tshl@163.com](mailto:litanshi_tshl@163.com)  Department of Emergency, The First Medical Center to Chinese People's Liberation Army General Hospital, No. 28 Fuxing Road, Haidian District, Beijing City, 100853, China

\*These authors contributed equally to this work.

© 2022 The Author(s). Published by Informa UK Limited, trading as Taylor & Francis Group.

This is an Open Access article distributed under the terms of the Creative Commons Attribution-NonCommercial License (<http://creativecommons.org/licenses/by-nc/4.0/>), which permits unrestricted non-commercial use, distribution, and reproduction in any medium, provided the original work is properly cited.

process of various diseases, expressions of apoptosis and inflammation-related genes can be modulated by lncRNAs [10,12,13]. LncRNA nuclear paraspeckle assembly transcript 1 (NEAT1), a novel member of lncRNAs, has been reported to exert an effect on cancer and inflammation [12]. In detail, the upregulation of NEAT1 has been found to aggravate sepsis-induced acute kidney injury *via* targeting miR-204 [13]. Besides, NEAT1 has a potential effect on exacerbating the glomerular nephritis [14]. However, the detailed mechanism by which NEAT1 acts on the podocyte injury has not been comprehensively expounded.

The existing study has proved that lncRNAs function through modulating miRNAs that regulate the cleavage and translation of target genes [15]. As the regulator of gene expression, miRNAs also occupy the critical position in the progression of diseases including kidney dysfunction [16,17]. miR-23b-3p has been documented to mitigate the kidney injury and serve as the potential therapeutic target in diabetic nephropathy [18]. Furthermore, mRNA is mediated by miRNAs to influence the podocyte injury [19]. B-cell lymphoma-2 (Bcl-2) interacting protein 3 like (BNIP3L), belonging to the regulatory genes, has also been verified to be capable of regulating podocyte injury [20]. Nonetheless, the relationship among NEAT1, miR-23b-3p and BNIP3L still remains obscure. Therefore, in present study, a mouse podocyte injury model was established through treating MPC5 cells with ADR to figure out the effects of NEAT1 on podocyte injury and the underlying mechanism.

## Materials and methods

### Cell culture and treatment

The mouse podocyte cell line MPC5 (iCell-m081; icell, Shanghai, China) was used to establish an *in vitro* podocyte injury model under the guidance of a previous study [7]. Briefly, the cells were incubated in Roswell Park Memorial Institute (RPMI) 1640 Medium (31870082; Gibco, Carlsbad, CA, USA) supplemented with 10 U/ml of interferon- $\gamma$  (bs-0388P, Bioss, China), 10% fetal bovine serum (FBS; C0227; Beyotime, Shanghai, China) and 1% Penicillin-Streptomycin (ST488; Beyotime, Shanghai, China) with 5% CO<sub>2</sub> at 33 °C. Then, MPC5 cells were differentiated at 37 °C (free interferon- $\gamma$ ) with 5% CO<sub>2</sub>. Next, the podocyte injury model was established by treating cells with 5  $\mu$ g/ml ADR (D1515; Sigma-Aldrich, St. Louis, MO, USA) for 24 hours (h).

### Transfection

NEAT1 overexpression plasmid (oe-NEAT1) constructed with the pcDNA3.1 (+) vector (V79020; Invitrogen, Carlsbad, CA, USA) was transfected into cells. Some empty vectors transfected into cells were utilized as empty vector controls (EVCs). The plasmid vectors pGPU6 of short hairpin (sh) RNA targeting NEAT1 (shNEAT1; C02001), shNEAT negative control (shNEAT1-NC; C03002) and shBNIP3L (C02001), shBNIP3L negative control (shNC; C03002), as well as miR-23b-3p inhibitor (I; C09003) and miR-23b-3p inhibitor control (IC; C09003) were purchased from Gene Pharma (Shanghai, China). The sequences of these plasmids were listed in the Table 1. In detail, MPC5 cells ( $1 \times 10^5$  cells/well) were initially seeded in the 24-well plate to 80% confluence. With the help of the Lipofectamine 2000 transfection reagent (11668019; ThermoFisher, Waltham, MA, USA), MPC5 cells were separately transfected with the above plasmid vectors, miR-23b-3p inhibitor and inhibitor control. After transfection and incubation for 48 h, these cells were harvested.

### Target prediction and dual-luciferase reporter assay

The StarBase (<http://starbase.sysu.edu.cn>) was applied to predict the target gene. The possibly competitively binding sites between NEAT1 and miR-23b-3p and between miR-23b-3p and BNIP3L were separately predicted by StarBase and TargetScan V7.2 ([http://www.targetscan.org/vert\\_72](http://www.targetscan.org/vert_72)) and then verified by dual-luciferase reporter assay.

To test whether NEAT1 targets miR-23b-3p and miR-23b-3p targets BNIP3L, the wild-type NEAT1 (NEAT1-WT; sequence: 5'-CCCUAACCUUGGGCAUGCAUCUUUAUAA-3') and BNIP3L (BNIP3L-WT; sequence: 5'-UUUGUCUGUUUCUAAAUGUGAA-3') reporter plasmids were constructed with pmirGLO luciferase vector (E1330; Promega, Madison, WI, USA). The mutant reporter plasmids for NEAT1 (NEAT1-MUT; sequence: 5'-CCCUAACCUUGGGC

**Table 1.** Sequences for transfection.

Gene	Sequence
shNEAT1 sense	5'-GGGUCAUCUUACUAGUAACA-3'
shNEAT1 antisense	5'-UUAUCUAGUAAGAUGACCCAG-3'
shNEAT1-NC sense	5'-UAGCAUCAGAUUGAGCCAUU-3'
shNEAT1-NC antisense	5'-UAGUCUACAUUGCAGCAGUA-3'
shBNIP3L sense	5'-CAAUGGUUCUGUAACUAUAGC-3'
shBNIP3L antisense	5'-UAUAGUUACAGAACCAUUGUG-3'
shBNIP3L NC sense	5'-GUAGUCCAUUGACUUUACAG-3'
shBNIP3L NC antisense	5'-GUUCAUAGAUUGACAUACUG-3'
miR-23b-3p inhibitor	5'-GGTAATCCCTGGCAATGTGAT-3'
miR-23b-3p inhibitor NC	5'-AAGTGCTCGCAGATTTGT-3'

AUGCAUCAUUGUAAG-3') and BNIP3L (BNIPL-MUT; sequence: 5'-UUUGUCUGUUUCUAAAGUGAGUA-3') were constructed with Phusion Site-Directed Mutagenesis Kit (F541; Thermo Fisher, Waltham, MA, USA).

$5 \times 10^3$  MPC5 cells were inoculated into the 24-well plate and transfected with the wild-type or mutant luciferase reporter plasmids, followed by transfection with miR-23b-3p inhibitor or inhibitor control and shBNIP3L or shBNIP3L negative control using Lipofectamine 2000 (11668019; ThermoFisher, Waltham, MA, USA). Following 48-h transfection, the activities of firefly luciferase and *Renilla* luciferase were detected using dual-luciferase reporter assay system (E1910; Promega, Madison, WI, USA) and observed by a GloMax<sup>®</sup> Explorer Multimode Microplate Reader (GM3500; Promega, Madison, WI, USA). The activity of firefly luciferase was normalized to that of *Renilla* luciferase.

### RNA immunoprecipitation (RIP) assay

RIP assay was conducted using RIP kit (Bes5101, BersinBio, China). After lysing the MPC5 cells, cell lysates were centrifuged to remove the DNA. Then, the cell lysates were incubated with magnetic beads conjugated with anti-Argonaute 2 antibody (AGO2, #2897, cell signaling technology, USA) or anti-IgG antibody (#2729, cell signaling technology, USA) at 4°C overnight. The RNA/antibody complex was washed with RIP buffer supplemented with RNase inhibitor and Proteinase K. RNA was extracted from the precipitate using Trizol reagent (T9424; Sigma-Aldrich, St. Louis, MO, USA). The immunoprecipitated RNA was analyzed by quantitative real-time polymerase chain reaction (qRT-PCR).

### Cell counting kit-8 (CCK-8) assay

In the present study, the CCK-8 assay was performed to measure cell viability. The cells were seeded in 96-well plates at a density of  $5 \times 10^3$  cells/well and cultured for 24 h. Later, the cells were added with 10  $\mu$ L CCK-8 solution (CK04; Dojindo, Kumamoto, Japan) and then were incubated for 4 h in the dark. Finally, the absorbance was measured with an iMark<sup>™</sup> microplate absorbance reader (E1140; Beyotime, Shanghai, China) at a wavelength of 450 nm and recorded.

### Flow cytometry

The apoptosis of MPC5 cells was determined using Annexin V-FITC/propidium iodide (PI) cell apoptosis kit

(V13242; Invitrogen, Carlsbad, CA, USA), and all the operations were performed under the guidance of manufacturer's instructions.  $1 \times 10^6$  cells were seeded in the 6-well plate and cultured for 24 h. Followed by being resuspended in 100  $\mu$ L binding buffer, cells at a concentration of  $1 \times 10^6$  cells/ml were obtained. Next, 5  $\mu$ L FITC Annexin V and 5  $\mu$ L PI working solution were used to incubate cells at room temperature for 15 min (min) away from the light. The apoptosis of MPC5 cells was measured by Attune NxT Flow Cytometer (A24858; Invitrogen, Carlsbad, CA, USA) and data were analyzed with the Attune NxT Flow Cytometer software (version 2.5; Invitrogen, Carlsbad, CA, USA).

### RNA isolation and quantitative real-time polymerase chain reaction (qRT-PCR)

Trizol reagent and MagMAX<sup>™</sup> mirVana<sup>™</sup> Total RNA Isolation Kit (A27828; Thermo Fisher, Waltham, MA, USA) were separately used to extract the RNAs and miRNAs from cells which were then preserved at  $-80^\circ\text{C}$ . The Nano Drop 2000 biological spectrometer (ND-2000; Thermo Fisher, Waltham, MA, USA) was employed to measure the concentration of total RNAs. With the assistance of TruScript<sup>™</sup> First Strand cDNA Synthesis Kit (54420; Norgen Biotek, Ontario, Canada), complementary DNAs (cDNAs) were synthesized from 1  $\mu$ g of total RNAs. QRT-PCR experiment was carried out with Fast SYBR<sup>™</sup> Green Master Mix (4385610; Thermo Fisher, Waltham, MA, USA) under QuantStudio<sup>™</sup> 7 Flex Real-Time PCR System (4485701; Thermo Fisher, Waltham, MA, USA). The primers used in this study are listed in Table 2. The conditions of qRT-PCR were listed as follows: 95°C for 5 min, and 40 cycles of 95°C for 15 seconds (s), 58°C for 30s and 74°C for 30s. The  $2^{-\Delta\Delta\text{CT}}$  calculation method was applied to quantify the expressions of relative genes [21].

### Western blot

The relative protein expression levels of genes related to podocyte injury, apoptosis and epithelial-mesenchymal transition (EMT), including Bcl-2, Bcl-2 associated X (Bax), Cleaved (C)-caspase-3, Epithelial (E)-cadherin, Neural(N)-

**Table 2.** Primer for qRT-PCR.

	Forward primer (5'→3')	Reverse primer (5'→3')
NEAT1	GGCCTCCAGACTTTGCAAAA	CATACACACGCCTAACACCG
MiR-23b-3p	GAGCATCACATTGCCAGGG	GTGCAGGGTCCGAGGT
BNIP3L	CTGGAGCACGTTCTTCTC	ACAGTGCGAACTGCCTCTTG
GAPDH	AGGTCGGTGTGAACGGATTG	GGGGTCGTTGATGGCAACA
U6	CTCGCTTCGGCAGCAC	AACGCTTACGAATTTGCGT

cadherin, Vimentin, Snail, Wilms' tumor 1 (WT1), Nephlin, Desmin and BNIP3L, were determined by western blot as previously described [20]. Briefly, after being rinsed by phosphate-buffered saline (PBS; ST476; Beyotime, Shanghai, China) and harvested, cells were lysed and extracted with Radio Immunoprecipitation Assay (RIPA; R0278; Sigma-Aldrich, St. Louis, MO, USA) lysis buffer. The relative protein concentration was measured by Bicinchoninic acid (BCA) protein kit (BCA1; Sigma-Aldrich, St. Louis, MO, USA). The protein samples were electrophoresed by sodium dodecyl sulfate-polyacrylamide gel electrophoresis (SDS-PAGE; P0690; Beyotime, Shanghai, China) and then transferred into polyvinylidene fluoride (PVDF; FFP33; Beyotime, Shanghai, China) membrane. Followed by being blocked with 5% skimmed milk at room temperature for 2 h, the membrane was incubated with primary antibodies comprising anti-WT1 antibody (ABIN3021698, 52 kDa, 1:1000) purchased from antibodies-online (Aachen, Germany), as well as anti-Nephlin antibody (ab136894, 134 kDa, 1:1000), anti-Desmin antibody (ab32362, 53 kDa, 1:1000), anti-BNIP3L antibody (ab109414, 24 kDa, 1:1000), anti-Bcl-2 antibody (ab182858, 26 kDa, 1:1000), anti-Bax antibody (ab32503, 21 kDa, 1:1000), anti-Cleaved (C)-caspase-3 antibody (ab49822, 17 kDa, 1:1000), anti-E-cadherin antibody (ab231303, 97 kDa, 1:1000), anti-N-cadherin antibody (ab18203, 100 kDa, 1:1000), anti-Vimentin antibody (ab92547, 54 kDa, 1:1000), anti-Snail antibody (ab82846, 29 kDa, 1:1000), and anti-GAPDH antibody (ab181602, 36 kDa, 1:1000) purchased from Abcam (Cambridge, UK) at 4 °C overnight. The internal reference in this research was GAPDH. Thereafter, the membrane was further cultivated with goat anti-rabbit secondary antibody (ab205718, 1:2000; Abcam, Cambridge, UK) and goat anti-mouse secondary antibody (ab205719, 1:2000; Abcam, Cambridge, UK) at room temperature for 1 h. Then, the membrane was rinsed by Tris-buffered saline Tween (TBST; ab64204; Abcam, Cambridge, UK), and incubated utilizing enhanced chemiluminescence (ECL) kit (ab65623; Abcam, Cambridge, UK) for visualizing. After the membrane was exposed under iBright™ CL1500 Imaging System (A44240; Invitrogen, Carlsbad, CA, USA), the gray value of all protein bands was quantified by ImageJ (version 5.0; Bio-Rad, Hercules, CA, USA).

### Statistical analysis

All the experiments of this study were repeated three times, the data of which were described as mean ± standard deviation (SD). Statistical analyses were implemented in SPSS 22.0 (IBM Cor., Armonk, NY, USA). One-way analysis of variance (ANOVA) was the method determining

the statistical significances followed by Dunnett's *post hoc* test.  $p < 0.05$  was defined as statistical significance.

## Results

### *Oe-NEAT1 enhanced the promoting effect of ADR on NEAT1 while shNEAT1 had the opposite effect*

The expression level of lncRNA NEAT1 was measured by qRT-PCR after the establishment of model and transfection. As described in Figure 1A, the level of lncRNA NEAT1 was upregulated by ADR (Figure 1A,  $p < 0.001$ ). Oe-NEAT1 further promoted while shNEAT1 dwindled the expression level of NEAT1 in ADR-treated MPC5 cells (Figure 1A,  $p < 0.01$ ).

### *Oe-NEAT1 enhanced the inhibitory effect of ADR on cell viability while shNEAT1 had the opposite effect*

The cell viability was measured by CCK-8 assay. In line with Figure 1B, the cell viability of MPC-5 was significantly suppressed in ADR group (Figure 1B,  $p < 0.001$ ). Compared with ADR + EVC group, the cell viability was markedly decreased in ADR + NEAT1 group but was notably increased in ADR + shNEAT1 group (Figure 1B,  $p < 0.05$ ). The results implied that oe-NEAT1 enhanced while shNEAT1 dampened the inhibitory effect of ADR on cell viability.

### *Oe-NEAT1 downregulated the levels of podocyte injury markers (WT1, nephrin) but upregulated that of another marker (desmin) while shNEAT1 generated the opposite effects*

The protein expression levels of the podocyte injury markers were measured by western blot [22]. As the data depicted in the Figure 1C and 1D, compared to Blank group, WT1 and Nephlin expressions were diminished while Desmin expression was elevated in ADR group (Figure 1C and 1D,  $p < 0.001$ ). Compared to ADR + EVC group, WT1 and Nephlin expressions were downregulated but Desmin expression was upregulated in ADR + NEAT1 group, while the inverse changing trends were observed in ADR + shNEAT1 group (Figure 1C and 1D,  $p < 0.05$ ). To conclude, oe-NEAT1 downregulated the levels of podocyte injury markers (WT1 and Nephlin) but upregulated that of another marker (Desmin), whereas the opposite changing trends were noticed under the transfection of shNEAT1.

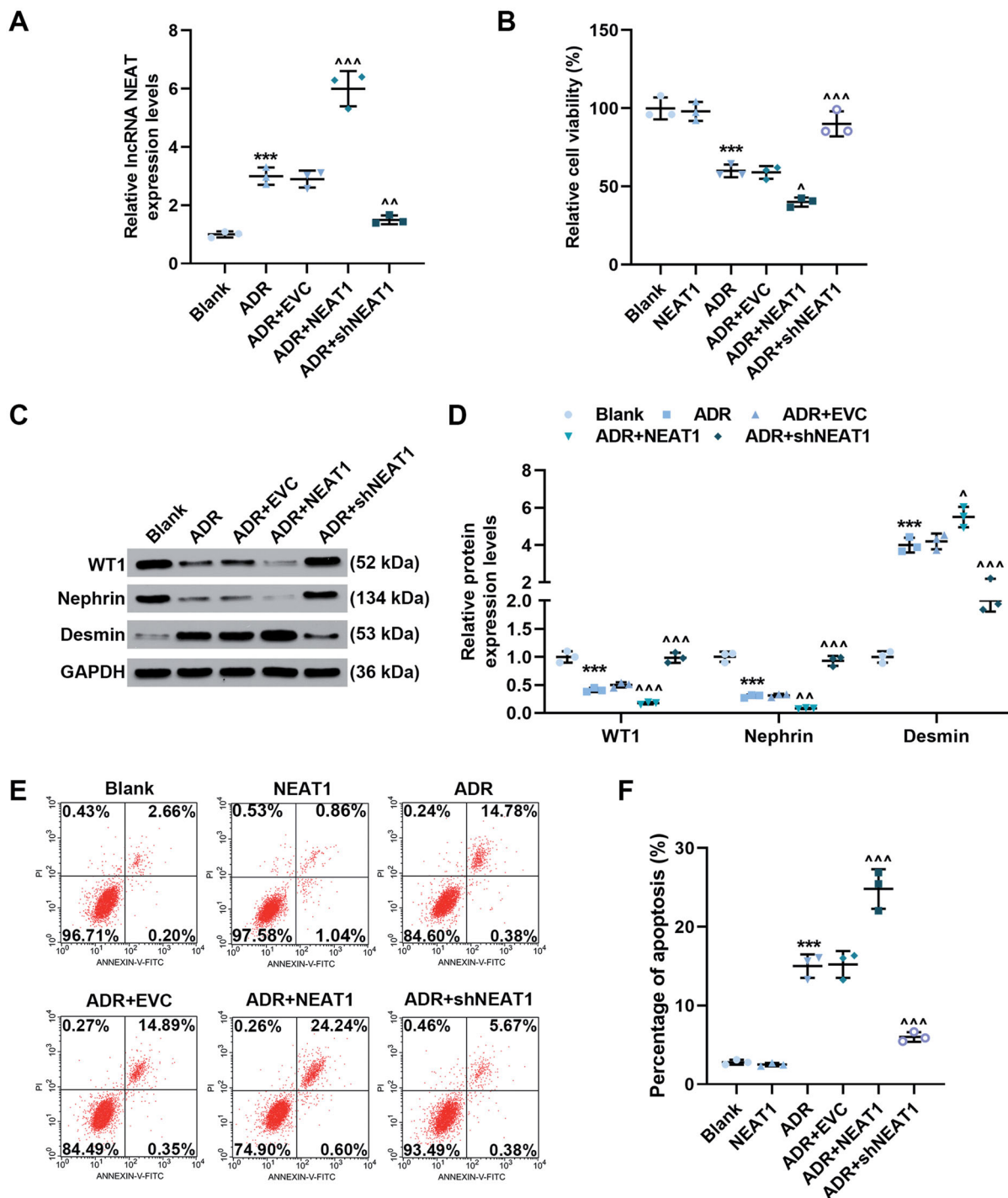


**Figure 1.** NEAT1 overexpression enhanced the effects of ADR on promoting NEAT1 expression, apoptosis and marker (Desmin) level and on suppressing cell viability and podocyte markers (WT1, Nephrin) levels, while shNEAT1 had the opposite effects. The experiment was divided into 5 or 6 groups: blank group (podocytes were cultured normally), NEAT1 group (podocytes were transfected with NEAT1 overexpression plasmid), ADR group (podocytes were treated with 5  $\mu$ g/ml doxorubicin for 24 h), ADR + EVC group (podocytes were transfected with EVCs and treated with 5  $\mu$ g/ml doxorubicin for 24 h), ADR + NEAT1 group (podocytes were transfected with NEAT1 overexpression plasmid and treated with 5  $\mu$ g/ml doxorubicin for 24 h) and ADR + shNEAT1 group (podocytes were transfected with shNEAT1 and treated with 5  $\mu$ g/ml doxorubicin for 24 h). (A) The expression level of NEAT1 was detected by qRT-PCR and the internal reference was GAPDH. (B) The viability of MPC5 cells in six groups was measured by CCK-8 assay. (C and D) The expression levels of podocyte injury makers including WT1, Nephrin and Desmin in the MPC5 cells in five groups were quantified by western blot and the internal reference was GAPDH. (E and F) The apoptosis rate of the MPC5 cells in six groups was detected by flow cytometry. All experiments were repeated three times. Experimental data were expressed by mean  $\pm$  standard deviation (SD) (\*\*\*)  $P < 0.001$ ;  $^{\circ}P < 0.05$ ,  $^{\wedge}P < 0.01$ ,  $^{\wedge\wedge}P < 0.001$ ; \*vs. Blank group;  $^{\circ}$ vs. ADR + EVC group) (NEAT1: nuclear paraspeckle assembly transcript 1; shNEAT1: short hairpin NEAT1; qRT-PCR: quantitative real-time polymerase chain reaction; MPC5: mouse podocyte cell line; CCK-8; Cell Counting Kit 8; EVC: empty vector control; WT1: Wilms' tumor 1).

### ***Oe-NEAT1 facilitated ADR-induced apoptosis in mouse podocyte injury model while shNEAT1 acted contrarily***

The flow cytometry was applied to detect the cell apoptosis in the ADR-induced mouse podocyte injury model. As shown in Figure 1E and 1F, the apoptosis rate of MPC5 cells in ADR group was obviously higher than that in blank group (Figure 1E and 1F,  $p < 0.001$ ). Compared to ADR + EVC group, the apoptosis of cells in ADR + NEAT1 group was further augmented, but that in ADR + shNEAT1 group was lessened (Figure 1E and 1F,  $p < 0.001$ ). Collectively, oe-NEAT1 promoted ADR-induced apoptosis in mouse podocyte injury model while shNEAT1 had the opposite effect.

### ***MiR-23b-3p could competitively bind with NEAT1***

StarBase was applied to predict the target gene and the competitively binding sites between NEAT1 and miR-23b-3p. As presented in Figure 2A, the potential target of NEAT1 was miR-23b-3p. Thereafter, the dual-luciferase reporter assay was conducted to test this prediction with the results displayed in the Figure 2B. The luciferase activity was higher in NEAT1-WT + I group than in NEAT1-WT + IC group (Figure 2B,  $p < 0.001$ ). However, there were no obvious changes concerning luciferase activity between NEAT1-MUT + I group and NEAT1-MUT + IC group, indicating that NEAT1 directly targeted miR-23b-3p. Then, RIP assay was performed with an antibody against AGO2 in MPC5 cells. The results demonstrated that NEAT1 and miR-23b-3p were signally enriched by the AGO2 antibody (Figure 2C,  $p < 0.001$ ), again confirming that NEAT1 directly targeted miR-23b-3p.

### ***MiR-23b-3p inhibitor reversed the effects of shNEAT1 on the expression of miR-23b-3p***

As shown in Figure 2D, oe-NEAT1 diminished the expression of miR-23b-3p in untreated MPC5 cells ( $p < 0.001$ ). In addition, as compared to the ADR + shNEAT1-NC group, the expression of miR-23b-3p in ADR + shNEAT1 group was upregulated (Figure 2E,  $p < 0.001$ ). In comparison with the ADR + I group, the expression of miR-23b-3p in ADR + shNEAT1 + I group was also upregulated (Figure 2E,  $p < 0.001$ ).

### ***MiR-23b-3p inhibitor downregulated the levels of podocyte injury markers (WT1, nephrin), upregulated that of another marker (desmin) and impaired the effects of shNEAT1 on podocyte injury markers***

Western blot was also applied to detect the protein expression levels of podocyte injury markers when

MPC5 cells were transfected with miR-23b-3p inhibitor and shNEAT1. As the Figure 2F and 2G illustrated, relative to ADR + shNEAT1-NC group, ADR + shNEAT1 group had upregulated protein levels of WT1 and Nephrin and downregulated protein level of Desmin (Figure 2F and 2G,  $p < 0.001$ ). Compared to ADR + IC group, the protein expression levels of WT1 and Nephrin were negatively regulated and that of Desmin was positively regulated in ADR + I group (Figure 2F and 2G,  $p < 0.01$ ). Besides, compared to ADR + shNEAT1 group, ADR + shNEAT1 + I group exhibited suppressed protein levels of WT1 and Nephrin and promoted protein level of Desmin, while the opposite results were obtained in ADR + shNEAT1 + I group when comparing to ADR + I group (Figure 2F and 2G,  $p < 0.01$ ). In a word, miR-23b-3p inhibitor downregulated the levels of podocyte injury markers (WT1, Nephrin), upregulated that of another marker (Desmin) and reversed the effects of shNEAT1 on podocyte injury markers.

### ***MiR-23b-3p inhibitor weakened the effects of shNEAT1 on promoting cell viability in ADR-induced podocyte injury model***

The cell viability was detected by the CCK-8 assay. According to Figure 2H, cell viability was obviously stronger in ADR + shNEAT1 group than in ADR + shNEAT1-NC group. Compared to ADR + IC group, cell viability in ADR + I group was suppressed ( $p < 0.01$ ). Besides, the cell viability in ADR + shNEAT1 + I group was higher than that in ADR + I group but was lower than that in ADR + shNEAT1 group ( $p < 0.01$ ). Altogether, miR-23b-3p inhibitor reversed the effects of shNEAT1 on promoting the cell viability in ADR-induced podocyte injury model.

### ***MiR-23b-3p inhibitor offset the inhibitory effects of shNEAT1 on cell apoptosis in ADR-induced mouse podocyte injury model***

The apoptosis of MPC5 cells transfected with miR-23b-3p inhibitor and shNEAT1 was also examined. Compared to ADR + shNEAT1-NC group, the apoptosis rate in ADR + shNEAT1 group was decreased, and relative to ADR + IC group, the apoptosis rate was increased in ADR + I group (Figure 2I and 2J,  $p < 0.001$ ). Besides, ADR + shNEAT1 + I group exhibited promoted apoptosis rate compared to ADR + shNEAT1 group, whilst presenting lessened apoptosis rate compared to ADR + I group (Figure 2I and 2J,  $p < 0.01$ ). It can be concluded that miR-23b-3p inhibitor weakened the inhibitory effects of shNEAT1 on cell apoptosis in ADR-induced mouse podocyte injury model.

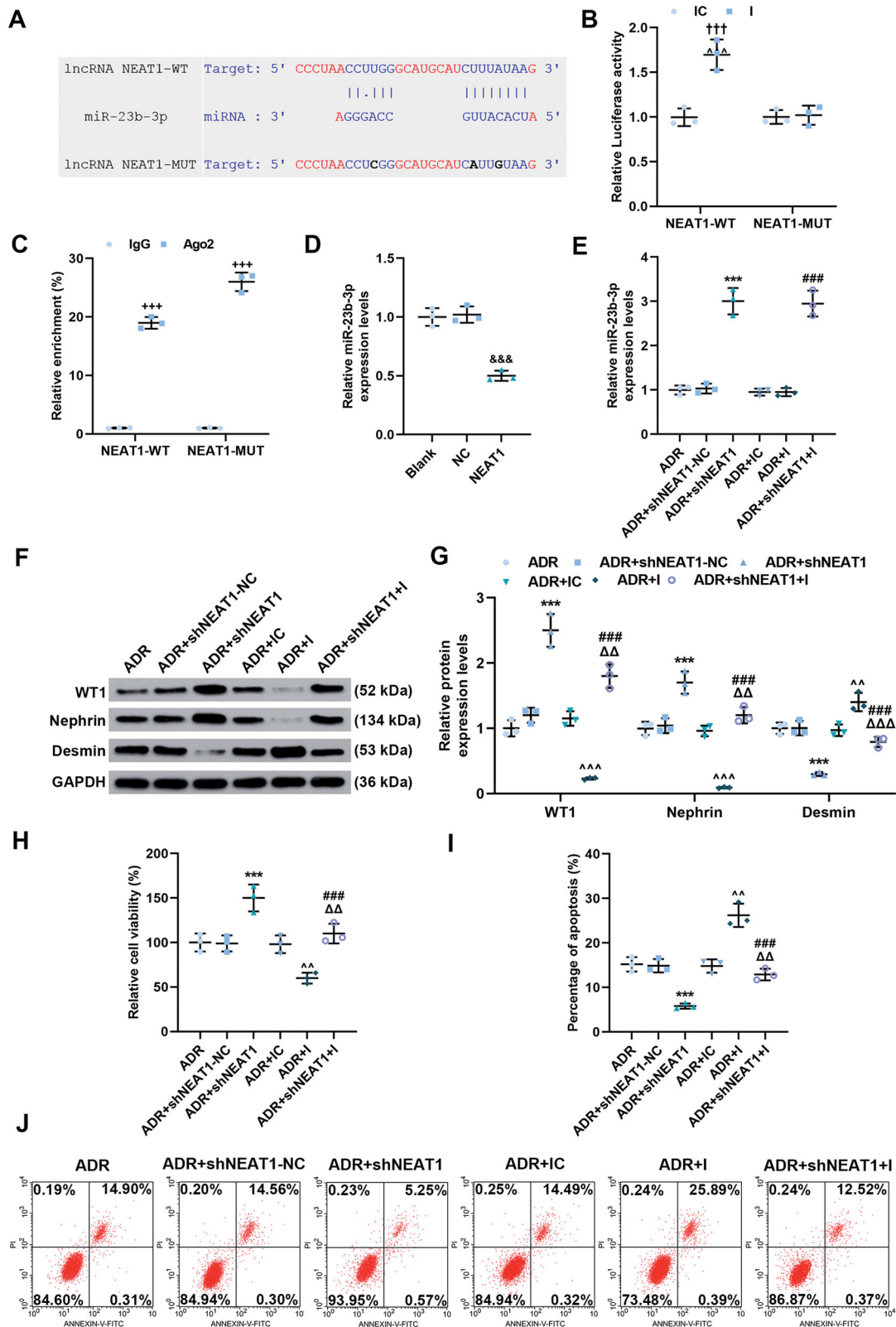


**Figure 2.** NEAT1 targeted miR-23b-3p, and miR-23b-3p inhibitor downregulated the levels of podocyte markers WT1 and Nephrin, upregulated that of marker Desmin and reversed the effects of shNEAT1 on cell viability and apoptosis. (A and B) Target prediction of NEAT1 was conducted by StarBase and tested by dual-luciferase reporter assay. (C) RIP assay was conducted by immunoprecipitation of anti-Ago2 antibody and anti-IgG antibody. The expressions of NEAT1 and miR-23b-3p were detected by qRT-PCR. (D) The mRNA expression level of miR-23b-3p in MPC5 cells transfected with NEAT1 overexpression plasmid or NC was quantified by qRT-PCR and the internal reference was U6. For (E–J), the experiment was divided into 6 groups: ADR group (podocytes were treated with 5  $\mu$ g/ml doxorubicin for 24 h), ADR + shNEAT1-NC group (podocytes were transfected with shNEAT1-NC

### miR-23b-3p directly targeted BNIP3L

The target gene of miR-23b-3p was predicted by TargetScan and the complementary binding sites between miR-23b-3p and BNIP3L were listed in Figure 3A. Then, this prediction was tested by dual-luciferase reporter assay (Figure 3B). According to the results, the luciferase activity was enhanced in BNIP3L-WT+I group compared to that in BNIP3L-WT-IC group (Figure 3B,  $p < 0.01$ ), and there was no obvious difference of luciferase activity between BNIP3L-MUT+IC group and BNIP3L-MUT+I group, indicating that miR-23b-3p directly targeted BNIP3L. In addition, RIP assay was conducted with the incubation of an antibody against AGO2 with MPC5 cells. The findings demonstrated that BNIP3L and miR-23b-3p were prominently enriched by the AGO2 antibody (Figure 3C,  $p < 0.001$ ), further affirming that BNIP3L directly targeted miR-23b-3p.

### BNIP3L expression was upregulated in ADR-induced podocyte injury model

The protein and mRNA expression levels were quantified using western blot and qRT-PCR, respectively. From Figure 3D–3F, it turned out that the expression level of BNIP3L was higher in ADR group than in Blank group, reflecting that BNIP3L was highly expressed in ADR-induced podocyte injury model (Figure 3D–3F,  $p < 0.001$ ).

### ShBNIP3L impaired the effects of miR-23b-3p inhibitor on BNIP3L expression

In line with Figure 3G–3I, compared to IC+shNC+ADR group, the expression level of BNIP3L was upregulated in ADR+I+shNC group but was downregulated in IC+shBNIP3L+ADR group (Figure 3G–3I,  $p < 0.01$ ). Besides, the expression level

of BNIP3L in I+shBNIP3L+ADR group was lower than that in I+shNC+ADR group yet was higher than that in IC+shBNIP3L+ADR group (Figure 3G–3I,  $p < 0.01$ ). In addition, NEAT1 overexpression promoted the expression of BNIP3L only in podocytes induced by ADR, but not in normal podocytes (Supplementary Figure 1). To sum up, shBNIP3L reversed the effects of miR-23b-3p inhibitor on expression of BNIP3L.

### ShBNIP3L upregulated the levels of podocyte injury markers (WT1, nephrin), downregulated that of another marker (desmin) and offset the effects of miR-23b-3p inhibitor on podocyte injury markers

Western blot was conducted to quantitate the protein expression levels of podocyte injury makers. As the Figure 3J and 3K illustrated, compared to IC+shNC+ADR group, the protein expression levels of WT1 and Nephrin were negatively regulated but that of Desmin was positively regulated in I+shNC+ADR group (Figure 3J and 3K,  $p < 0.01$ ). In contrast to IC+shNC+ADR group, the protein expression levels of WT1 and Nephrin were increased but that of Desmin was decreased in IC+shBNIP3L+ADR group (Figure 3J and 3K,  $p < 0.01$ ). Besides, in I+shBNIP3L+ADR group, the protein expression levels of WT1 and Nephrin were elevated but that of Desmin was dwindled when compared to those in I+shNC+ADR group, whereas inverse results were obtained when comparing I+shBNIP3L+ADR group with IC+shBNIP3L+ADR group (Figure 3J and 3K,  $p < 0.05$ ). Collectively, shBNIP3L upregulated the levels of podocyte injury markers WT1 and Nephrin, downregulated that of another marker Desmin and partly reversed the effects of miR-23b-3p inhibitor on podocyte injury markers.

#### Figure 2. (Continued)

and treated with 5  $\mu\text{g/ml}$  doxorubicin for 24 h), ADR+shNEAT1 group (podocytes were transfected with shNEAT1 and treated with 5  $\mu\text{g/ml}$  doxorubicin for 24 h), ADR+IC group (podocytes were transfected with miR-23b-3p inhibitor control and treated with 5  $\mu\text{g/ml}$  doxorubicin for 24 h), ADR+I group (podocytes were transfected with miR-23b-3p inhibitor and treated with 5  $\mu\text{g/ml}$  doxorubicin for 24 h) and ADR+shNEAT1+I group (podocytes were co-transfected with shNEAT1 and miR-23b-3p inhibitor and treated with 5  $\mu\text{g/ml}$  doxorubicin for 24 h). (E) The mRNA expression level of miR-23b-3p in MPC5 cells in six groups was quantified by qRT-PCR and the internal reference was U6. (F and G) The expression levels of podocyte injury makers including WT1, Nephrin and Desmin in MPC5 cells in six groups were quantified by western blot and the internal reference was GAPDH. (H) The viability of MPC5 cells in six groups was assessed by CCK-8. (I and J) The apoptosis rate of MPC5 cells in six groups was detected by flow cytometry. All experiments were repeated three times. Experimental data were expressed by mean  $\pm$  standard deviation (SD) ( $^{+++}p < 0.001$ ;  $^{+++}p < 0.001$ ;  $^{\&\&}p < 0.001$ ;  $^{***}p < 0.001$ ;  $^{###}p < 0.001$ ;  $^{\wedge\wedge}p < 0.01$ ,  $^{\wedge\wedge\wedge}p < 0.001$ ;  $^{\Delta\Delta}p < 0.01$ ,  $^{\Delta\Delta\Delta}p < 0.001$ ;  $^{\dagger}$ vs. IC group;  $^{+}$ vs. IgG group;  $^{\&}$ vs. NC group;  $^{*}$ vs. ADR+shNEAT1-NC group;  $^{\#}$ vs. ADR+I group;  $^{\Delta}$ vs. ADR+shNEAT1 group;  $^{\circ}$ vs. ADR+IC group). (NEAT1: nuclear paraspeckle assembly transcript 1; ADR: adriamycin; shNEAT1: short hairpin NEAT1; shNEAT1-NC: shNEAT1 negative control; I; miR-23b-3p inhibitor; IC; miR-23b-3p negative control; qRT-PCR: quantitative real-time polymerase chain reaction; MPC5: mouse podocyte cell line; CCK-8; Cell Counting Kit 8; WT1: Wilms' tumor 1).



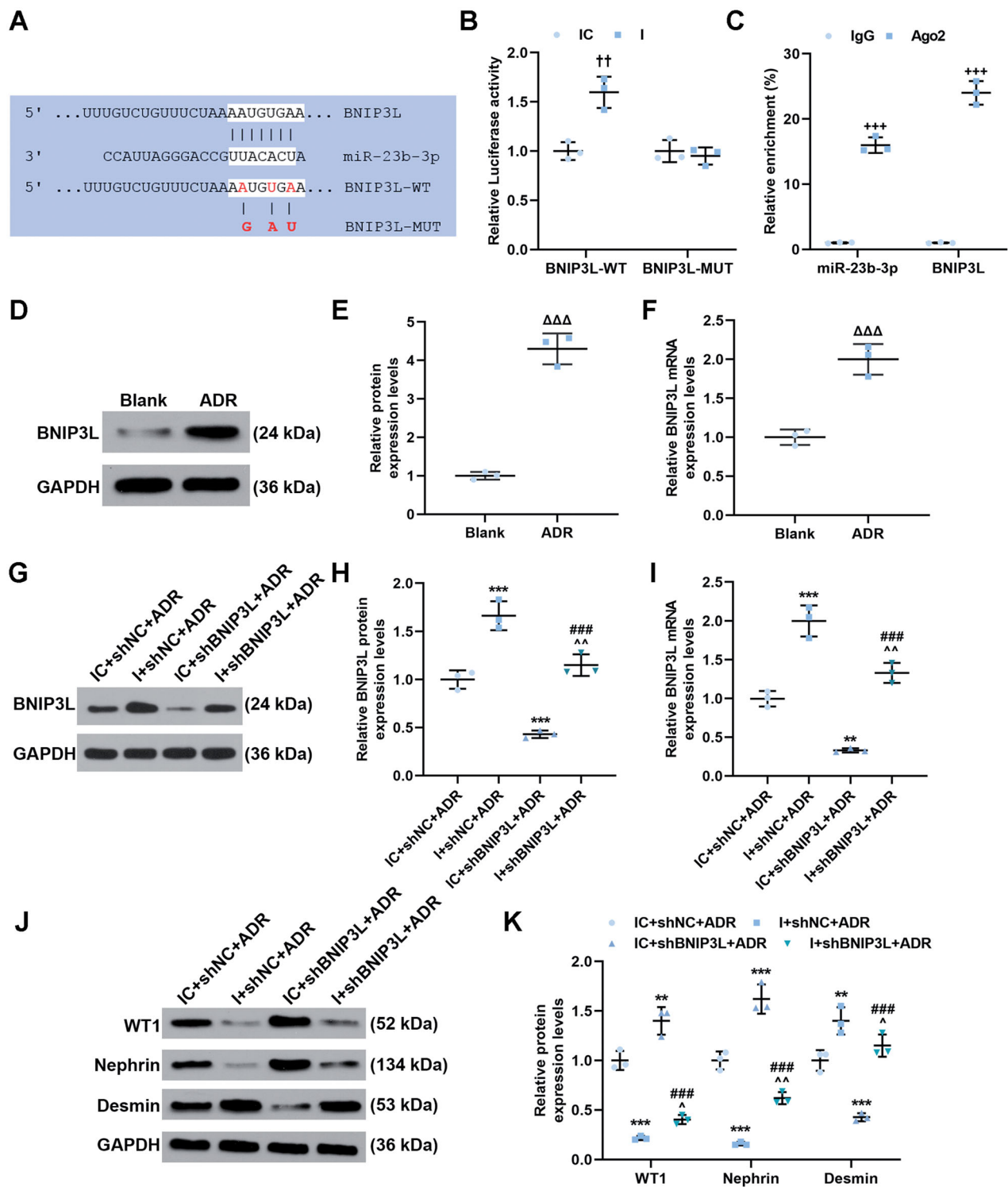


**Figure 3.** MiR-23b-3p targeted BNIP3L, and shBNIP3L upregulated the levels of podocyte markers WT1 and Nephrin, downregulated that of marker Desmin and reversed the effects of miR-23b-3p inhibitor on BNIP3L expression. (A and B) Target prediction of miR-23b-3p was calculated by TargetScan V7.2 and tested by dual-luciferase reporter assay. (C) RIP assay was conducted by immunoprecipitation of anti-Ago2 antibody and anti-IgG antibody. The expressions of BNIP3L and miR-23b-3p were detected by qRT-PCR. (D–F) The expression level of BNIP3L in MPC5 cells treated with or without ADR was quantified by qRT-PCR and western blot and the internal reference was GAPDH. For (G–K), the experiment was divided into 4 groups: ADR + IC + shNC group (podocytes were co-transfected with shNC and miR-23b-3p inhibitor control and treated with 5  $\mu$ g/ml doxorubicin for 24 h), ADR + I + shNC group (podocytes were co-transfected with shNC and miR-23b-3p inhibitor and treated with 5  $\mu$ g/ml doxorubicin for 24 h), ADR + IC + shBNIP3L group (podocytes were co-transfected with shBNIP3L and miR-23b-3p inhibitor control and treated with 5  $\mu$ g/ml doxorubicin for 24 h), and ADR + I + shBNIP3L group (podocytes were co-transfected with shBNIP3L and miR-23b-3p

### **ShBNIP3L reversed the effects of miR-23b-3p inhibitor on suppressing cell viability and promoting apoptosis in ADR-induced podocyte injury model**

The viability of MPC-5 cells was detected by CCK-8 assay. Compared to MPC-5 cell viability in IC + shNC + ADR group, the viability was decreased in I + shNC + ADR group but was increased in IC + shBNIP3L + ADR group (Figure 4A,  $p < 0.01$ ). In I + shBNIP3L + ADR group, the viability of MPC-5 cells was higher than that in I + shNC + ADR group but was lower than that in IC + shBNIP3L + ADR group (Figure 4A,  $p < 0.05$ ). It can be summarized that shBNIP3L reversed the inhibitory effects of miR-23b-3p on MPC-5 cell viability in ADR-induced podocyte injury model.

The apoptosis of MPC-5 cells was also evaluated. By contrast with IC + shNC + ADR group, I + shNC + ADR group had increased apoptosis rate but IC + shBNIP3L + ADR group had decreased one (Figure 4B and 4C,  $p < 0.001$ ). In I + shBNIP3L + ADR group, the apoptosis rate was lower than that in I + shNC + ADR group but was higher than that in IC + shBNIP3L + ADR group (Figure 4B and 4C,  $p < 0.01$ ), manifesting that shBNIP3L reversed the promoting effect of miR-23b-3p on MPC-5 cell apoptosis in ADR-induced podocyte injury model.

### **ShBNIP3L promoted bcl-2 level, inhibited bax and C-caspase-3 levels and offset the effects of miR-23b-3p inhibitor on genes related to apoptosis**

The protein expression levels of the genes related to apoptosis were measured through western blot (Figure 4D and 4E). Relative to the protein levels in IC + shNC + ADR group, the protein level of Bcl-2 was downregulated and those of Bax and C-caspase-3 were upregulated in I + shNC + ADR group (Figure 4D and 4E,  $p < 0.01$ ). In contrast to IC + shNC + ADR group, IC + shBNIP3L + ADR group had elevated protein level of Bcl-2 and diminished protein levels of Bax and C-caspase-3 (Figure 4D and 4E,  $p < 0.001$ ). Besides, in I + shBNIP3L + ADR group, the protein expression level of Bcl-2 was higher than that in I + shNC + ADR group

but was lower than that in IC + shBNIP3L + ADR group, while the protein expression levels of Bax and C-caspase-3 were lower than those in I + shNC + ADR group but were higher than those in IC + shBNIP3L + ADR group (Figure 4D and 4E,  $p < 0.05$ ). Collectively, shBNIP3L promoted Bcl-2 expression, inhibited Bax and C-caspase-3 expressions and reversed the effects of miR-23b-3p inhibitor on genes related to apoptosis

### **ShBNIP3L augmented E-cadherin level, lessened N-cadherin, vimentin and snail levels and weakened the effects of miR-23b-3p inhibitor on genes related to EMT**

The protein expression levels of the genes related to EMT in MPC-5 cells were also measured by western blot (Figure 4F and 4G). As compared to IC + shNC + ADR group, the protein expression levels of N-cadherin, Vimentin and Snail were increased and that of E-cadherin was decreased in I + shNC + ADR group (Figure 4F and 4G,  $p < 0.05$ ). When compared with IC + shNC + ADR group, IC + shBNIP3L + ADR group had downregulated N-cadherin, Vimentin and Snail levels and upregulated E-cadherin level (Figure 4F and 4G,  $p < 0.01$ ). Besides, in I + shBNIP3L + ADR group, the protein expression level of E-cadherin was higher than that in I + shNC + ADR group but was lower than that in IC + shBNIP3L + ADR group, whereas the protein expression levels of N-cadherin, Vimentin and Snail were lower than those in I + shNC + ADR group but were higher than those in IC + shBNIP3L + ADR group (Figure 4F and 4G,  $p < 0.05$ ). Given the above findings, shBNIP3L promoted E-cadherin expression, inhibited N-cadherin, Vimentin and Snail expressions and reversed the effects of miR-23b-3p inhibitor on genes related to EMT.

## **Discussion**

The reduction of podocyte number symbolizes podocyte injury and the apoptosis of podocyte is one of main causes for the loss of podocytes [23]. There are

#### **Figure 3. (Continued)**

inhibitor and treated with 5  $\mu\text{g/ml}$  doxorubicin for 24 h). (G–I) The expression level of BNIP3L in MPC5 cells in four groups was quantified by qRT-PCR and western blot (J–K) The expression levels of podocyte injury makers including WT1, Nephlin and Desmin in MPC5 cells in four groups were quantified by qRT-PCR and western blot and the internal reference was GAPDH. All experiments were repeated three times. Experimental data were expressed by mean  $\pm$  standard deviation (SD) ( $^{\dagger\dagger}P < 0.01$ ;  $^{\dagger\dagger\dagger}P < 0.001$ ;  $^{\Delta\Delta\Delta}P < 0.001$ ;  $^{**}P < 0.01$ ,  $^{***}P < 0.001$ ;  $^{\#\#\#}P < 0.001$ ;  $^{\circ}P < 0.05$ ,  $^{\wedge\wedge\wedge}P < 0.01$ ;  $^{\dagger}$ vs. IC group;  $^{+}$ vs. IgG group;  $^{\Delta}$ vs. blank group;  $^{*}$ vs. IC + shNC + ADR group;  $^{\#}$ vs. IC + shBNIP3L + ADR group;  $^{\circ}$ vs. I + shNC + ADR group) (BNIP3L: B-cell lymphoma-2 interacting protein 3 like; ADR: adriamycin; MPC5: mouse podocyte cell line; I; miR-23b-3p inhibitor; IC; miR-23b-3p negative control; shBNIP3L: short hairpin BNIP3L; shNC: shBNIP3L negative control; qRT-PCR: quantitative real-time polymerase chain reaction; WT1: Wilms' tumor 1).

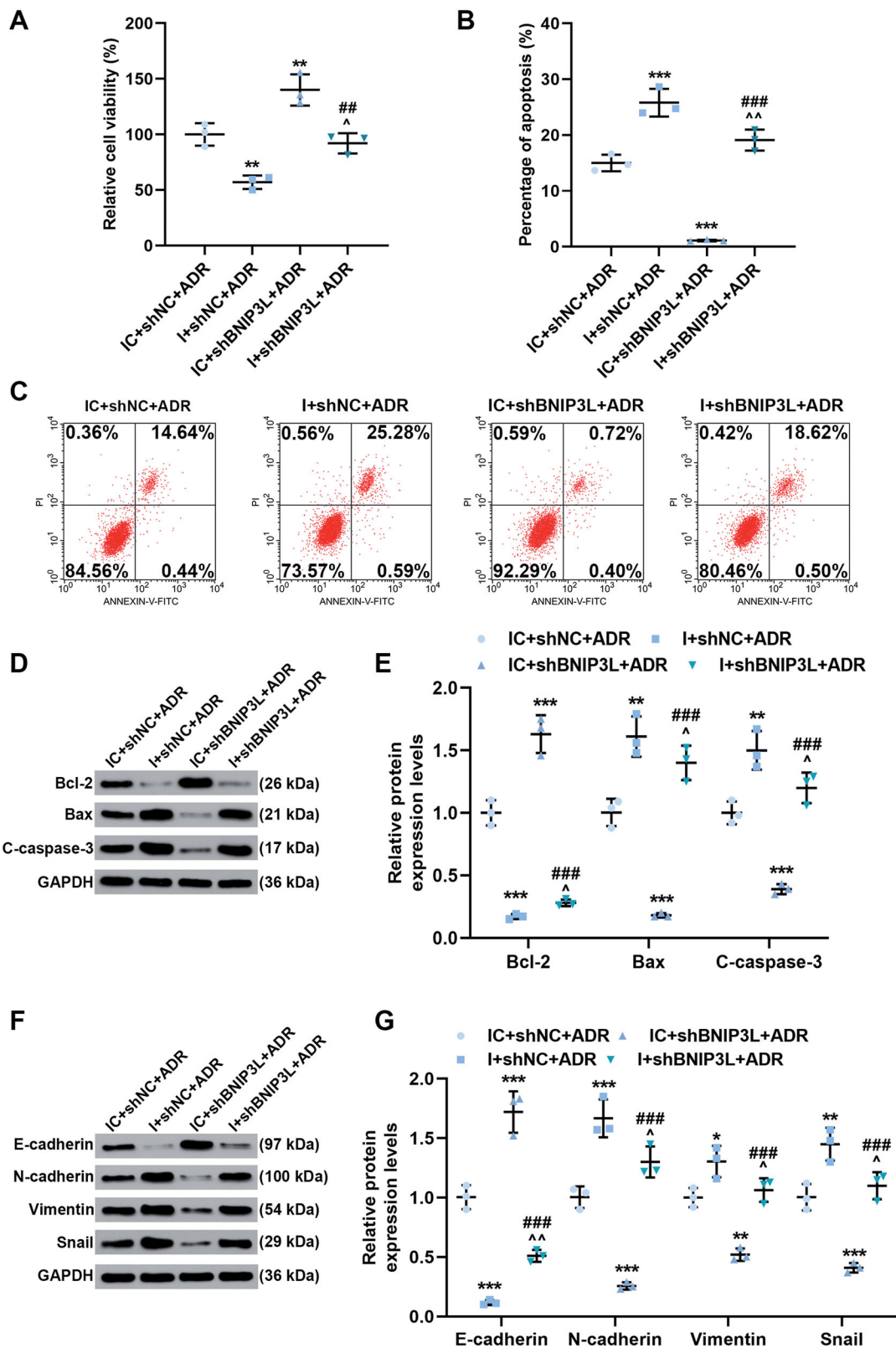


**Figure 4.** ShBNIP3L reversed the cell viability inhibition and apoptosis promotion induced by miR-23b-3p inhibitor and regulated the expressions of genes related to apoptosis and EMT. The experiment was divided into 4 groups: ADR + IC + shNC group (podocytes were co-transfected with shNC and miR-23b-3p inhibitor control and treated with 5  $\mu$ g/ml doxorubicin for 24 h), ADR + I + shNC group (podocytes were co-transfected with shNC and miR-23b-3p inhibitor and treated with 5  $\mu$ g/ml doxorubicin for 24 h), ADR + IC + shBNIP3L group (podocytes were co-transfected with shBNIP3L and miR-23b-3p inhibitor control and treated with 5  $\mu$ g/ml doxorubicin for 24 h), and ADR + I + shBNIP3L group (podocytes were co-transfected with shBNIP3L and miR-23b-3p inhibitor and treated with 5  $\mu$ g/ml doxorubicin for 24 h). (A) The viability of MPC5 cells in four groups was detected with CCK-8

some markers of podocyte injury including WT1, Nephlin and Desmin [22]. WT1 is a significant factor for podocytes to maintain the homeostasis, the downregulation of which would induce the apoptosis of podocytes [24]. Nephlin is another vital factor that can inhibit the apoptosis of podocytes and help podocytes recover from injury [25,26]. On the contrary, the expression of Desmin is in company with the process of podocyte loss [24]. Moreover, as an anti-tumor antibiotic, ADR could not only inhibit the tumor but also cause the irreparable damage to the podocytes [27]. Therefore, the podocyte injury models were always constructed by the ADR [28,29]. Recently, the regulating function of NEAT1 on the apoptosis of myocytes, smooth muscle cells and renal tubular epithelial cells has been documented [30–32]. But there are few papers discussing the effects of NEAT1 on podocyte injury. Thus, this study probed into the effects of NEAT1 on viability and apoptosis of podocytes in the ADR-induced mouse podocyte injury model. According to the experimental results, NEAT1 was high-expressed in ADR-induced podocyte model, which reduced the viability and promoted the apoptosis of podocytes in ADR-induced mouse podocyte injury model. Also, the markers of podocyte damage were regulated by NEAT1. Specifically, WT1 and Nephlin levels were downregulated while Desmin level was upregulated by oe-NEAT1. These evidences suggest that NEAT1 promotes ADR-induced podocyte injury. Interestingly, we found that NEAT1 alone did not significantly affect podocyte apoptosis, but generated promoting effects on apoptosis when podocytes were treated with ADR, indicating that NEAT1 may only take effect under ADR-induced pathological conditions. Although the promoting function of NEAT1 on podocyte injury has been tested, the underlying mechanism awaited to be clarified.

As the previous study stated, the effects of lncRNAs were realized by targeting miRNAs [15]. In Alzheimer's disease, NEAT1 takes effect *via* targeting miR-124 [33]. In the process of acute kidney injury induced by sepsis, NEAT1 plays a vital part by regulating miR-204 [13].

However, the target miRNA of NEAT1 in podocyte injury remained obscure. Hence, the bioinformatics analysis by StarBase and the dual-luciferase reporter assay were performed, whose results indicated that NEAT1 directly targeted miR-23b-3p. As a recent study reported, miR-23b-3p modulates the apoptosis and autophagy of lens epithelial cells [24], which also has been confirmed to possess the protective function on podocyte injury [18]. Since the mechanism of the effects of miR-23b-3p is still unclear, the effects of miR-23b-3p on ADR-induced mouse podocyte injury model were detected in this study. The present research discovered that miR-23b-3p ameliorated the podocyte injury and reversed the effects of NEAT1, signifying that the effects of NEAT1 on podocyte injury were realized by regulating miR-23b-3p.

The effects of miRNAs were also fulfilled by modulating its target [34]. miR-23b-3p impacted the pancreatic ductal adenocarcinoma, hepatocellular carcinoma and cardiomyocyte hypoxia *via* targeting annexin A2, zinc-finger E-box-binding homeobox 1 and nuclear factor E2-related factor 2, respectively [35–37]. However, there were no documents about the target gene of miR-23b-3p in podocyte injury. According to the bioinformatics analysis by Targetscan and verification by dual-luciferase reporter assay, miR-23b-3p directly targeted BNIP3L. BNIP3L is a member of Bcl-2 family, whose upregulation can induce the cell apoptosis and necrosis [38]. Moreover, BNIP3L could enhance aldosterone-induced podocyte apoptosis and mitochondrial dysfunction through permeabilization of the mitochondrial outer membrane by mediating the intrinsic apoptotic pathway [20]. In the context of the indeterminate mechanism underlying the effects of BNIP3L, the role of BNIP3L in the process of podocyte injury was analyzed. The results revealed that BNIP3L exacerbated the podocyte injury and partly offset the effects of miR-23b-3p, manifesting that the effects of miR-23b-3p on podocyte injury were achieved *via* modulating BNIP3L. Nevertheless, the mechanism of these effects was still undiscovered so that the factors related to apoptosis were detected.

#### Figure 4. (Continued)

kit. (B and C) The apoptosis of MPC5 cells in four groups was measured by flow cytometry. (D and E) The protein expression levels of genes related to apoptosis including Bcl-2, Bax and C-caspase-3 in MPC5 cells in four groups were quantified by qRT-PCR and the internal reference was GAPDH. (F and G) The protein expression levels of genes related to EMT including E-cadherin, N-cadherin, Vimentin and Snail in MPC5 cells in four groups were quantified by qRT-PCR and the internal reference was GAPDH. All experiments were repeated three times. Experimental data were expressed by mean  $\pm$  standard deviation (SD) (\* $P < 0.05$ , \*\* $P < 0.01$ , \*\*\* $P < 0.001$ ;  $^{\circ}P < 0.05$ ,  $^{\wedge\wedge}P < 0.01$ ;  $^{\#}P < 0.01$ ,  $^{\#\#}P < 0.001$ ; \*vs. IC + shNC + ADR group;  $^{\circ}$ vs. I + shNC + ADR group;  $^{\#}$ vs. IC + shBNIP3L + ADR group) (BNIP3L: B-cell lymphoma-2 interacting protein 3 like; EMT: epithelial-mesenchymal transition; MPC5: mouse podocyte cell line; I; miR-23b-3p inhibitor; IC; miR-23b-3p negative control; shBNIP3L: short hairpin BNIP3L; shNC: shBNIP3L negative control; CCK-8; Cell Counting Kit 8; Bcl-2: B-cell lymphoma-2; C-caspase-3: Cleaved-caspase-3; Bax: Bcl-2 associated X; E-cadherin: Epithelial-cadherin; N-cadherin: Neural-cadherin; qRT-PCR: quantitative real-time polymerase chain reaction).

To further verify the above findings in molecular level, the impacts of miR-23b-3p and BNIP3L on the factors related to apoptosis were detected. Bcl-2 family serves a significant role in cell apoptosis [39]. As members of the Bcl-2 family, Bcl-2 has abilities in ameliorating apoptosis and Bax is capable of intensifying apoptosis [40]. In the podocyte injury, the downregulation of Bcl-2 and the increased ratio of Bax/Bcl-2 promote the apoptosis [41]. Furthermore, another mediator of cell apoptosis and death is caspase family [42]. Caspase-3, belonging to caspase family, exhibits upregulated expression in the apoptosis of podocytes [43]. The protein expressions of C-caspase-3, Bcl-2 and Bax are applied to detect and explain the cell apoptosis in podocyte injury [32]. In the present study, BNIP3L upregulated the expressions of Bax and C-caspase-3, downregulated that of Bcl-2 and partly reversed the effects of miR-23b-3p. Additionally, EMT is one of the responses of podocytes to injury resulting in the depletion of podocytes, and blocked EMT can alleviate the injury of podocytes [44]. The upregulation of N-cadherin and the downregulation of E-cadherin are hallmarks of EMT [45]. Besides, Vimentin can also serve as the biomarker of EMT [46]. During the progression of podocyte injury, EMT of the podocyte is mediated by Snail [44]. Therefore, these factors related to EMT were detected in this study, uncovering that BNIP3L downregulated E-cadherin level, upregulated N-cadherin, Vimentin and Snail levels and partly neutralized the effects of miR-23b-3p. In a word, the effects of BNIP3L and miR-23b-3p were realized by regulating the expressions of Bcl-2, Bax, C-caspase-3, E-cadherin, N-cadherin, Vimentin and Snail.

However, there are some aspects need to be optimized in our study. This paper figured out the effects of NEAT1 on podocyte injury, through verifying the target relationship among NEAT1, miR-23b-3p and BNIP3L and exploring the mechanism underlying the effects of NEAT1. But the relevant experiments only carried out in mouse model *in vitro*, so that experiments *in vivo* are necessary for further study. In addition, the collection of clinical samples to verify the expression level of NEAT1 in kidney tissue is also helpful to improve our conclusion.

In conclusion, in ADR-induced mouse podocyte injury model, miR-23b-3p inhibitor reverses the effects of shNEAT1 on promoting NEAT1 expression and cell viability and on hindering cell apoptosis, which is also positively correlated with the markers of podocyte injury. But shBNIP3L offsets the impacts of miR-23b-3p inhibitor. Furthermore, NEAT1 promotes the podocyte injury *via* targeting miR-23b-3p/BNIP3L axis. In detail, the effects of NEAT1 are realized by upregulating the expressions of Bax, C-caspase-3, N-cadherin, Vimentin

and Snail, and downregulating the expressions of Bcl-2 and E-cadherin. Taken together, NEAT1 modulates the podocyte injury *via* targeting miR-23b-3p/BNIP3L axis, which provides a new direction for targeted treatment of renal injury triggered by exposure to nephrotoxic drugs.

### Author contributions

Substantial contributions to conception and design: Jing Wang, Junpeng Luo. Data acquisition, data analysis and interpretation: Li Du, Xin Shu, Chengyu Guo, Tanshi Li. Drafting the article or critically revising it for important intellectual content: Jing Wang, Junpeng Luo. Final approval of the version to be published: Jing Wang, Junpeng Luo, Li Du, Xin Shu, Chengyu Guo, Tanshi Li. Agreement to be accountable for all aspects of the work in ensuring that questions related to the accuracy or integrity of the work are appropriately investigated and resolved: Jing Wang, Junpeng Luo, Li Du, Xin Shu, Chengyu Guo, Tanshi Li.

### Disclosure statement

The authors declare no conflicts of interest.

### Funding

This work was supported by the important and special project "Winter Olympic Emergency Medical Support" by Ministry of National science [2019YFF0302300]; the 13th Five-year Plan for Key Discipline Construction Project of PLA [A350109].

### Data availability statement

The analyzed data sets generated during the study are available from the corresponding author on reasonable request.

### References

- [1] Wang CS, Greenbaum LA. Nephrotic syndrome. *Pediatr Clin North Am*. 2019;66(1):73–85.
- [2] Sharma M, Mahanta A, Barman AK, et al. Acute kidney injury in children with nephrotic syndrome: a single-center study. *Clin Kidney J*. 2018;11(5):655–658.
- [3] Pollak MR. Inherited podocytopathies: FSGS and nephrotic syndrome from a genetic viewpoint. *J Am Soc Nephrol*. 2002;13(12):3016–3023.
- [4] Liu X, Cao W, Qi J, et al. Leonurine ameliorates adriamycin-induced podocyte injury via suppression of oxidative stress. *Free Radic Res*. 2018;52(9):952–960.
- [5] Nagata M. Podocyte injury and its consequences. *Kidney Int*. 2016;89(6):1221–1230.
- [6] Guan N, Ren YL, Liu XY, et al. Protective role of cyclosporine a and minocycline on mitochondrial disequilibrium-related podocyte injury and proteinuria

- occurrence induced by adriamycin. *Nephrol Dial Transplant*. 2015;30(6):957–969.
- [7] Yang X, Wu D, Du H, et al. MicroRNA-135a is involved in podocyte injury in a transient receptor potential channel 1-dependent manner. *Int J Mol Med*. 2017;40(5):1511–1519.
- [8] Hu M, Wang R, Li X, et al. LncRNA MALAT1 is dysregulated in diabetic nephropathy and involved in high glucose-induced podocyte injury via its interplay with  $\beta$ -catenin. *J Cell Mol Med*. 2017;21(11):2732–2747.
- [9] Zhou Z, Wan J, Hou X, et al. MicroRNA-27a promotes podocyte injury via PPAR $\gamma$ -mediated  $\beta$ -catenin activation in diabetic nephropathy. *Cell Death Dis*. 2017;8(3):e2658–e2658.
- [10] Chen S, Liang H, Yang H, et al. LincRNA-p21: function and mechanism in cancer. *Med Oncol*. 2017;34(5):98.
- [11] Troy A, Sharpless NE. Genetic "lnc"-age of noncoding RNAs to human disease. *J Clin Invest*. 2012;122(11):3837–3840.
- [12] Du M, Yuan L, Tan X, et al. The LPS-inducible lncRNA Mirt2 is a negative regulator of inflammation. *Nat Commun*. 2017;8(1):2049.
- [13] Chen Y, Qiu J, Chen B, et al. Long non-coding RNA NEAT1 plays an important role in sepsis-induced acute kidney injury by targeting miR-204 and modulating the NF- $\kappa$ B pathway. *Int Immunopharmacol*. 2018;59:252–260.
- [14] Huang YS, Hsieh HY, Shih HM, et al. Urinary xist is a potential biomarker for membranous nephropathy. *Biochem Biophys Res Commun*. 2014;452(3):415–421.
- [15] Paraskevopoulou MD, Hatzigeorgiou AG. Analyzing MiRNA-LncRNA interactions. *Methods Mol Biol*. 2016;1402:271–286.
- [16] Lu TX, Rothenberg ME. MicroRNA. *J Allergy Clin Immunol*. 2018;141(4):1202–1207.
- [17] Kato M, Natarajan R. microRNA Cascade in diabetic kidney disease: big impact initiated by a small RNA. *Cell Cycle*. 2009;8(22):3613–3614.
- [18] Zhao B, Li H, Liu J, et al. MicroRNA-23b targets ras GTPase-activating protein SH3 domain-binding protein 2 to alleviate fibrosis and albuminuria in diabetic nephropathy. *J Am Soc Nephrol*. 2016;27(9):2597–2608.
- [19] Zheng Z, Hu H, Tong Y, et al. MiR-27b regulates podocyte survival through targeting adenosine receptor 2B in podocytes from non-human primate. *Cell Death Dis*. 2018;9(11):1133.
- [20] Guo Y, Deng X, Chen S, et al. MicroRNA-30e targets BNIP3L to protect against aldosterone-induced podocyte apoptosis and mitochondrial dysfunction. *Am J Physiol Renal Physiol*. 2017;312(4):F589–F598.
- [21] Zhuang ST, Cai YJ, Liu HP, et al. LncRNA NEAT1/miR-185-5p/IGF2 axis regulates the invasion and migration of Colon cancer. *Mol Genet Genomic Med*. 2020;8(4):e1125.
- [22] Doublie S, Lupia E, Catanuto P, et al. Testosterone and 17 $\beta$ -estradiol have opposite effects on podocyte apoptosis that precedes glomerulosclerosis in female estrogen receptor knockout mice. *Kidney Int*. 2011;79(4):404–413.
- [23] Lu CC, Wang GH, Lu J, et al. Role of podocyte injury in glomerulosclerosis. *Adv Exp Med Biol*. 2019;1165:195–232.
- [24] Zhou L, Chen X, Lu M, et al. Wnt/ $\beta$ -catenin links oxidative stress to podocyte injury and proteinuria. *Kidney Int*. 2019;95(4):830–845.
- [25] Matoba K, Kawanami D, Nagai Y, et al. Rho-Kinase blockade attenuates podocyte apoptosis by inhibiting the notch signaling pathway in diabetic nephropathy. *IJMS*. 2017;18(8):1795.
- [26] Verma R, Venkatarreddy M, Kalinowski A, et al. Nephron is necessary for podocyte recovery following injury in an adult mature glomerulus. *PLOS One*. 2018;13(6):e0198013.
- [27] Sai YP, Song YC, Chen XX, et al. Protective effect of astragalosides from radix astragali on adriamycin-induced podocyte injury. *Exp Ther Med*. 2018;15(5):4485–4490.
- [28] Yi M, Zhang L, Liu Y, et al. Autophagy is activated to protect against podocyte injury in adriamycin-induced nephropathy. *Am J Physiol Renal Physiol*. 2017;313(1):F74–F84.
- [29] Zhang HT, Wang WW, Ren LH, et al. The mTORC2/akt/NF $\kappa$ B pathway-mediated activation of TRPC6 participates in Adriamycin-induced podocyte apoptosis. *Cell Physiol Biochem*. 2016;40(5):1079–1093.
- [30] Jiang X, Li D, Shen W, et al. LncRNA NEAT1 promotes hypoxia-induced renal tubular epithelial apoptosis through downregulating miR-27a-3p. *J Cell Biochem*. 2019;120(9):16273–16282.
- [31] Chen L, Wu X, Zeb F, et al. Acrolein-induced apoptosis of smooth muscle cells through NEAT1-Bmal1/clock pathway and a protection from asparagus extract. *Environ Pollut*. 2020;258:113735.
- [32] Yan H, Liang H, Liu L, et al. Long noncoding RNA NEAT1 sponges miR-125a-5p to suppress cardiomyocyte apoptosis via BCL2L12. *Mol Med Rep*. 2019;19(5):4468–4474.
- [33] Zhao MY, Wang GQ, Wang NN, et al. The long-non-coding RNA NEAT1 is a novel target for Alzheimer's disease progression via miR-124/BACE1 axis. *Neurol Res*. 2019;41(6):489–497.
- [34] Wu C, Zhao Y, Liu Y, et al. Identifying miRNA-mRNA regulation network of major depressive disorder in ovarian cancer patients. *Oncol Lett*. 2018;16(4):5375–5382.
- [35] Wei DM, Dang YW, Feng ZB, et al. Biological effect and mechanism of the miR-23b-3p/ANXA2 axis in pancreatic ductal adenocarcinoma. *Cell Physiol Biochem*. 2018;50(3):823–840.
- [36] Yang T, He X, Chen A, et al. LncRNA HOTAIR contributes to the malignancy of hepatocellular carcinoma by enhancing epithelial-mesenchymal transition via sponging miR-23b-3p from ZEB1. *Gene*. 2018;670:114–122.
- [37] Zhang R, Li Y, Liu X, et al. FOXO3a-mediated long non-coding RNA LINC00261 resists cardiomyocyte hypoxia/reoxygenation injury via targeting miR23b-3p/NRF2 axis. *J Cell Mol Med*. 2020;24(15):8368–8378.
- [38] Chen Y, Lewis W, Diwan A, et al. Dual autonomous mitochondrial cell death pathways are activated by

- nix/BNip3L and induce cardiomyopathy. *Proc Natl Acad Sci USA*. 2010;107(20):9035–9042.
- [39] Bruckheimer EM, Cho SH, Sarkiss M, et al. The bcl-2 gene family and apoptosis. *Adv Biochem Eng Biotechnol*. 1998;62:75–105.
- [40] Gao H, Dong H, Li G, et al. Combined treatment with acetazolamide and cisplatin enhances chemosensitivity in laryngeal carcinoma hep-2 cells. *Oncol Lett*. 2018;15(6):9299–9306.
- [41] Qiu L-Q, Sinniah R, I-Hong Hsu S. Downregulation of bcl-2 by podocytes is associated with progressive glomerular injury and clinical indices of poor renal prognosis in human IgA nephropathy. *J Am Soc Nephrol*. 2004;15(1):79–90.
- [42] Tsapras P, Nezis IP. Caspase involvement in autophagy. *Cell Death Differ*. 2017;24(8):1369–1379.
- [43] Lei X, Zhang L, Li Z, et al. Astragaloside IV/lncRNA-TUG1/TRAF5 signaling pathway participates in podocyte apoptosis of diabetic nephropathy rats. *Drug Des Devel Ther*. 2018;12:2785–2793.
- [44] Dou Y, Shang Y, Shen Y, et al. Baicalin alleviates adriamycin-induced focal segmental glomerulosclerosis and proteinuria by inhibiting the Notch1-Snail axis mediated podocyte EMT. *Life Sci*. 2020;257:118010.
- [45] Loh C-Y, Chai J, Tang T, et al. The E-Cadherin and N-Cadherin switch in epithelial-to-mesenchymal transition: signaling, therapeutic implications, and challenges. *Cells*. 2019;8(10):1118.
- [46] Zeisberg M, Neilson EG. Biomarkers for epithelial-mesenchymal transitions. *J Clin Invest*. 2009;119(6):1429–1437.